Received: 8 July 2023 | Revised: 7 November 2023 | Accepted: 18 December 2023

DOI: 10.1002/ajpa.24897

AMERICAN JOURNAL OF BIOLOGICAL ANTHROPOLOGY
The Official Journal of the American Association of Biological Anthropologists

WILEY

TECHNICAL NOTE

Technical note: A volumetric method for measuring the longitudinal arch of human tracks and feet

Kevin G. Hatala[1] | Stephen M. Gatesy[2] | Armita R. Manafzadeh[2,3,4,5] | Elizabeth M. Lusardi[1] | Peter L. Falkingham[6]

[1]Department of Biology, Chatham University, Pittsburgh, Pennsylvania, USA

[2]Department of Ecology, Evolution, and Organismal Biology, Brown University, Providence, Rhode Island, USA

[3]Institute for Biospheric Studies, Yale University, New Haven, Connecticut, USA

[4]Department of Earth and Planetary Sciences, Yale University, New Haven, Connecticut, USA

[5]Peabody Museum of Natural History, Yale University, New Haven, Connecticut, USA

[6]School of Biological and Environmental Sciences, Liverpool John Moores University, Liverpool, UK

Correspondence
Kevin G. Hatala, Department of Biology, Chatham University, Pittsburgh, PA, USA.
Email: kevin.g.hatala@gmail.com

Funding information
National Science Foundation, Grant/Award Numbers: BCS-1824821, BCS-1825403

Abstract

Fossil footprints (i.e., tracks) were believed to document arch anatomical evolution, although our recent work has shown that track arches record foot kinematics instead. Analyses of track arches can thereby inform the evolution of human locomotion, although quantifying this 3-D aspect of track morphology is difficult. Here, we present a volumetric method for measuring the arches of 3-D models of human tracks and feet, using both Autodesk Maya and Blender software. The method involves generation of a 3-D object that represents the space beneath the longitudinal arch, and measurement of that arch object's geometry and spatial orientation. We provide relevant tools and guidance for users to apply this technique to their own data. We present three case studies to demonstrate potential applications. These include, (1) measuring the arches of static and dynamic human feet, (2) comparing the arches of human tracks with the arches of the feet that made them, and (3) direct comparisons of human track and foot arch morphology throughout simulated track formation. The volumetric measurement tool proved robust for measuring 3-D models of human tracks and feet, in static and dynamic contexts. This tool enables researchers to quantitatively compare arches of fossil hominin tracks, in order to derive biomechanical interpretations from them, and/or offers a different approach for quantifying foot morphology in living humans.

KEYWORDS
fossil footprints, longitudinal arch, tracks

1 | INTRODUCTION

1.1 | The evolution of arched feet

For at least the past century, paleoanthropologists and comparative anatomists have allocated significant attention to studying the emergence and evolution of our foot's longitudinally arched morphology (Morton, 1924). Humans are the only extant primate with this foot anatomy, so it has been assumed that it must be uniquely well suited for bipedal locomotor functions. Recent studies have reshaped our understandings of whether and how the longitudinally arched configuration of our foot skeleton contributes to the demands of human bipedalism, and of which aspects of foot anatomy enable functions typically attributed to the longitudinal arch (e.g., Holowka et al., 2021; Kelly et al., 2014, 2015; Venkadesan et al., 2020; Welte et al., 2018, 2021). Some have proposed that a longitudinally arched foot may be more important for facilitating foot function during running than it is during walking (e.g., Holowka & Lieberman, 2018; Stearne et al., 2016). Still there remains great interest in understanding the evolution of arched feet in modern humans.

It is very difficult, however, to understand longitudinal arch anatomy from skeletal fossils. Part of that difficulty stems from the fact

that the arch is supported by several soft tissue elements, which typically do not fossilize. The bones that do fossilize are often fragmentary and/or found in isolation. Some researchers have hypothesized arch anatomies for fossil hominins based on just one or two bones, but others who have analyzed the same elements with different methods have found conflicting results (DeSilva & Throckmorton, 2010; Drapeau & Harmon, 2013; Prang, 2015; Venkadesan et al., 2020; Ward et al., 2011).

Fossil footprints (i.e., tracks) have been viewed as a potentially more viable path for reconstructing arch morphology. Tracks preserve records of the complete, articulated feet of fossil hominins during life. Their longitudinally arched shapes have been interpreted as direct images of plantar foot anatomy, and part of the excitement about hominin track discoveries has been the assumption that they record longitudinally arched foot anatomies in early hominins from the Pliocene and early Pleistocene. The longitudinal arches of the ~3.66 Ma footprints from Laetoli, Tanzania garnered attention following their initial discovery (Day & Wickens, 1980; Leakey & Hay, 1979) and the same was true for the ~1.5 Ma footprints discovered near Ileret, Kenya (Bennett et al., 2009). Later studies similarly assumed that the depth of footprints in the region of the medial longitudinal arch in some way resembled the arch height of the feet that made them (e.g., Crompton et al., 2012; Hatala et al., 2016). However, Holocene trackways from Walvis Bay, Namibia, which span a range of substrate conditions, also demonstrated that the height and shape of arch impressions in one individual's tracks can vary according to the properties of the substrate they are walking on (Morse et al., 2013). Our most recent work has now demonstrated that the longitudinal arches of footprints rarely provide accurate records of foot anatomy, and that they instead represent an important record of foot kinematics (Hatala et al., 2023). The morphology of a track's arch varies across different substrates because one's foot moves differently when it is able to displace larger quantities of substrate (e.g., when it sinks deeper). Thus, even though we now understand that arched footprints are not faithful records of foot anatomy, they remain uniquely valuable for understanding the evolution of human locomotor kinematics.

1.2 | Methods for quantifying arch morphology

A variety of techniques for quantifying longitudinal arch morphology in living human feet have been developed for primarily clinical or sutorial purposes. The absolute or relative height of the medial longitudinal arch can be measured directly, using a variety of two-dimensional linear or angular measures (e.g., Williams & McClay, 2000). More recently, with the growth and availability of 3-D scanning technology, direct 3-D measurements have become more common. These methods have recently included statistical shape modeling to describe complete foot anatomy and variation, including that of the longitudinal arch (e.g., Schuster et al., 2021; Stanković et al., 2018).

Aside from direct foot measurement, clinicians and footwear designers have, for over a century, evaluated what they refer to as "footprints" to assess longitudinal arch morphology (McKenzie, 1909). Here, "footprints" are acquired by coating the plantar surface of a person's foot with paint or ink, and asking that person to walk or stand on paper to quantify how much of their foot contacts the ground. The exact nature of these measurements has changed over time, but most have focused on quantifying the 2-D area of foot contact beneath the longitudinal arch (i.e., the instep; for a brief review see Cavanagh & Rodgers, 1987). More recently, similar methods have also been used to measure high-resolution 3-D foot scans (Domjanic et al., 2015).

Fossil footprints (i.e., tracks) differ fundamentally from paint/ink prints, because they represent a 3-D record of a complex interaction in which the foot and substrate mutually moved and deformed. Many of the tracks known from the human fossil record are deep impressions that were formed as hominins walked through soft, deformable substrates. In a deep track, the foot sinks to the point where the entire plantar surface contacts and deforms the ground. In these cases, envisioning the 3-D track as a 2-D paint mark is difficult if not impossible, as it is unclear where on the track's continuous 3-D topography one could objectively designate borders to define a 2-D plantar foot outline. Historically, the presence/absence or the heights of arches within hominin tracks have usually been discussed in qualitative or relative terms (e.g., appearing higher or lower than in other hominin tracks or in modern human tracks) because there is no easy way to measure them directly. For example, the height of the navicular is impossible to identify with confidence, as the bone does not leave behind any clear landmark within track morphology. In the absence of available methods for measuring track arches, some have attempted the same types of measurements described above for paint/ink prints (Bennett et al., 2009). However, we do not believe that methods designed to measure the instep of paint/ink prints are most appropriate for 3-D tracks, given the fundamental differences between the two types of records and the mechanics of how they form.

Again, our recent biplanar X-ray experiments have revealed that the longitudinal arch of a track is shaped by the flow of sediment in response to foot kinematics, and that track arches do not accurately represent the longitudinal arch anatomies of the feet that created them (Hatala et al., 2018, 2021, 2023). Still, even though the longitudinal arch of a track is not a direct anatomical signal, quantification of this feature offers important evidence for understanding hominin foot kinematics (Hatala et al., 2023).

1.3 | A new, volumetric method for quantifying the arches of tracks and feet

Here, we present a new, 3-D volumetric approach that we developed for quantifying and comparing the longitudinal arches of tracks. This technique can also be applied to measure longitudinal arches from 3-D scans of human feet. In fact, we have applied the technique to measure and directly compare the arches of tracks with the arches of the feet that made them (Hatala et al., 2023). We note that we have slightly adjusted our calculations since our first presentation of this

measurement technique (Hatala et al., 2023). The new calculations do not change any of the results or conclusions from that prior publication. We found that the revised formula merely helps with applications of the measurement tool to marginal cases (i.e., tracks that are much shallower or much deeper than those we analyzed previously). We present this approach in detail below, and we provide all of the relevant software tools and instructions that will allow others to implement similar measurements in their own studies of hominin tracks and/or feet.

2 | MATERIALS AND METHODS

2.1 | Overview of the method

Our approach is based on polygonal track and foot models that could be derived from a variety of sources, such as photogrammetry, scanning (laser, structured light, CT), animation, or simulation. We sample the volume of space below the track/foot arch using a prism consisting of two parallel base and roof triangles connected by three perpendicular walls (Figure 1). The user interactively reshapes and positions the prism by registering virtual markers representing its base vertices at the center of the heel impression, and at the approximate positions of the first and fifth metatarsophalangeal joints. Wall height of the prism is then adjusted to ensure that the prism fully captures the arch (exact height is not important, since the portion of the prism that is above the track model will be subsequently removed). Calculating the Boolean intersection between a track/foot and the prism yields an arch model (Figure 1b,c), from which relative arch volume (RAV) and other parameters are derived (Table 1). Detailed instructions and links to scripts are provided for implementation in Autodesk Maya and Blender (see Data Availability statement), and we have provided assessments of inter- and intra-observer error (Supporting Information).

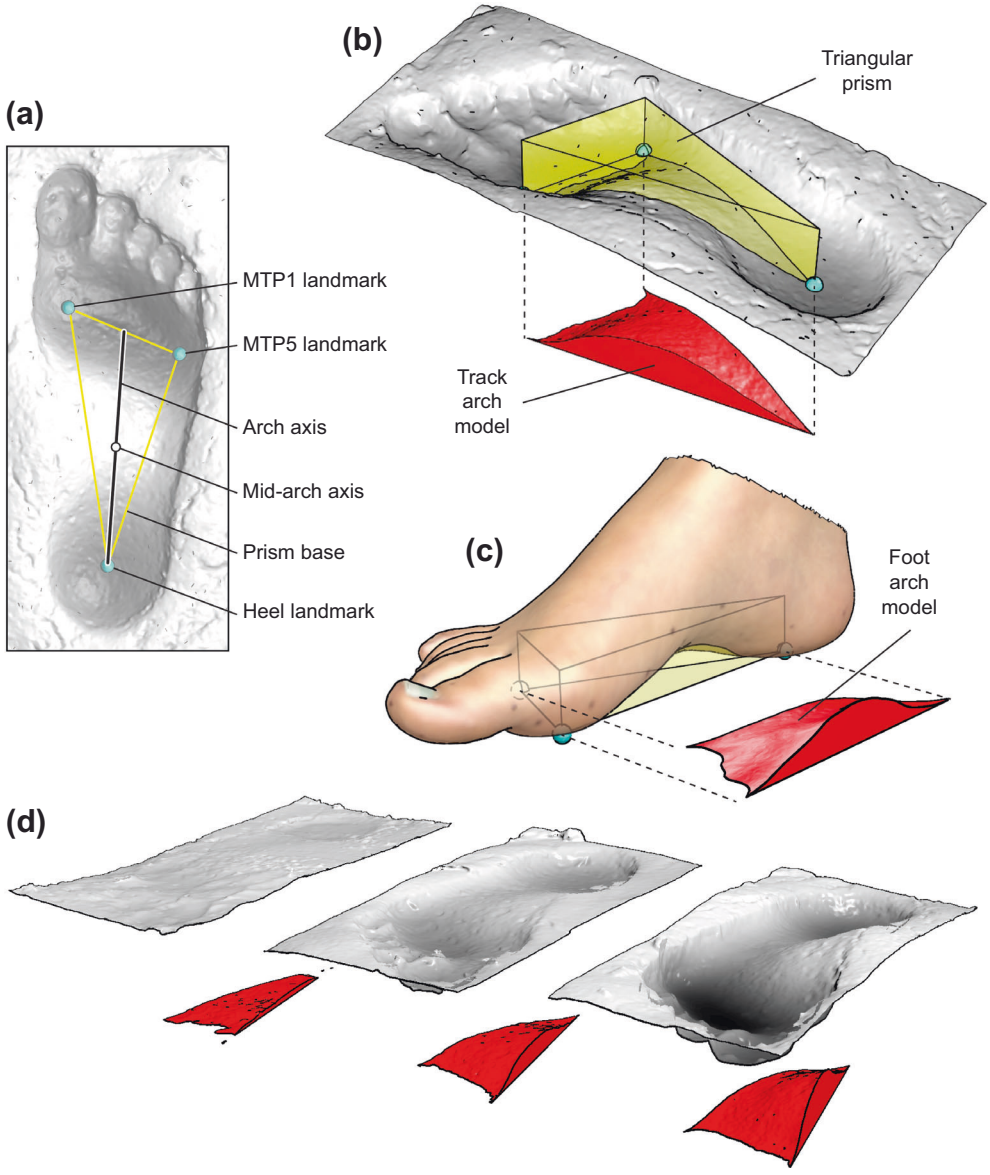

FIGURE 1 Boolean intersection between a triangular prism and a track/foot model yields an arch model. (a) Three landmarks (aqua spheres) placed at the center of the heel impression, and the approximate positions of the first and fifth metatarsophalangeal joints (MTP1 and MTP5, respectively) designate the prism's base. (b) A track arch model (red) samples the volume between landmarks and the deformed substrate. (c) A comparable foot arch model can be derived from static or dynamic plantar anatomy. (d) A sample of three tracks made by the same subject show, from left to right, increasing arch model volume (i.e., increasing relative arch volume) with increasing track depth.

TABLE 1 Aspects of arch model geometry measured in Maya and Blender scripts.

Variable	Description
Relative arch volume (RAV)	Arch volume, divided by ⅔ root of base area, expressed as a percentage (multiplied by 100)
Relative depth	Mid-axis depth, divided by axis length
Pitch	Pitch of arch axis, measured in degrees (heel deeper than forefoot results in positive pitch)
Roll	Roll of metatarsophalangeal (MTP) joint axis about arch axis, measured in degrees (external rotation of MTP joint axis results in positive roll)
Arch volume	Volume of arch model, measured in cm^3
Base area	Area of prism base, measured in cm^2
Axis length	Length from heel marker to midpoint of MTP joint axis, measured in cm
Mid-axis depth	Depth of arch axis at its midpoint, measured in cm
Side	Indicates whether the selected object was designated as a right or left foot or track

RAV was developed to measure both the concavity of a foot's anatomical arch, as well as the convexity of a track's corresponding morphology. Intuition about the meaning of specific RAV values is hampered by the triangular nature of the sampling geometry, but some examples can help. A RAV of 100 designates the volume of any completely filled prism having a wall height equal to the ⅔ root of its base area. A RAV of 25 is equivalent to an arch volume filling only one quarter of such a prism, a RAV of 10 filling one tenth, and so on (see Supporting Information for a more detailed explanation). Thus, RAV represents the average height of the arch object relative to the area of its base, expressed as a percentage:

$$\mathrm{RAV} = 100 * \left(\frac{\text{arch volume}}{\sqrt[\frac{2}{3}]{\text{base area}}} \right).$$

To help compare arch variables among hominin tracks that differ in absolute size (i.e., outline dimensions) and also in depth, we calculated relative depth. To do this, an arch axis was defined, spanning from the heel landmark to the midpoint of an axis drawn between the two metatarsophalangeal joint markers (Figure 1a). The absolute depth of the arch axis midpoint is measured and is then divided by the arch axis length. Relative depth provides an important measure of how much substrate was displaced relative to the hominin's foot size. We have seen previously that the RAVs of human tracks tend to increase as relative depth increases, and we have observed a logarithmic relationship between the two variables (Hatala et al., 2023). In other words, the same subject can produce tracks of different RAV, depending on how much substrate they displace when they make a given track (Figure 1d). We expect that other aspects of track morphology vary with relative depth as well, because depth-related trends have been observed across multiple other studies (e.g., Bennett & Morse, 2014; Morse et al., 2013).

2.2 | Case studies implementing volumetric arch measurement

Here, we provide three case studies of RAV implementation, using data collected during recently published experiments (Hatala et al., 2018, 2021, 2023). Full details of experimental protocols are available in those references and are summarized here. All experimental subjects provided their informed consent to participate, in accordance with protocols approved by the Institutional Review Boards of Brown University (Providence, RI, USA) and Chatham University (Pittsburgh, PA, USA).

In these experiments, between 85 and 115 lead beads 1.5 mm in diameter (with sticker backings) were affixed to subjects' right feet using medical adhesive. Marker numbers varied in different iterations of the experiment (one used 85, another used 115), as we chose to add more markers to the dorsal surface of the foot to enhance the resolution of our 3-D animations. Because the additional markers were added to the dorsum of the foot, resolution across the plantar surface (where arch measurements were taken) remained unchanged. Prior to their attachment, a template of bead locations was drawn on each subject's foot using a semi-permanent marker, and their foot was 3-D scanned using a structured light scanner. After scanning was complete, the lead beads were fixed to the marked locations. With beads attached to their feet, subjects stood or walked upon a variety of substrates for a minimum of 13 trials, each captured by biplanar X-ray video at 50 frames per second. For the first trial, each subject quietly stood in the field of biplanar X-ray view, and we captured an image of their static, weight-bearing foot. For at least three trials subjects walked at self-selected comfortable walking speeds across a rigid carbon fiber plank. For at least nine more trials, subjects walked at the same self-selected speeds across three muds of increasing compliance (minimum three trials per substrate). For mud trials, the footprints left behind were captured to render 3-D models using photogrammetry or a structured light scanner.

Following acquisition of experimental data, bead 3-D positions were tracked using XMALab software (Knörlein et al., 2016). Each subject's 3-D foot scan was imported to Autodesk Maya, and the tracked 3-D bead positions were used to animate their 3-D foot model as it moved and deformed within the calibrated biplanar X-ray space. These 3-D animations enabled visualization and direct quantification of foot motion and deformation throughout foot-substrate interactions in each trial (Hatala et al., 2021).

2.2.1 | Measuring arches of static and dynamic feet

In our first application, we measured the longitudinal arches of human feet under static and dynamic conditions. Using two forms of static data, we compared the same subjects' feet in unloaded and weight-bearing conditions. To do so, we first measured the 3-D foot scan models that were collected prior to bead attachment, while subjects rested their leg upon a stool. We then measured the animated 3-D foot models during static, quiet standing trials. As described above, deformations of the foot scan models were dictated by the real 3-D

bead location data acquired with biplanar X-ray. Measurements under these two conditions allowed us to evaluate the extent and nature of arch deformation that was induced by weight-bearing.

Next, we quantified dynamic arch morphology, as captured in each individual frame of biplanar X-ray video, while the same subjects walked across solid and deformable substrates. These quantifications relied upon frame-by-frame measurement of the 3-D animated foot in each trial. Using Autodesk Maya's "Create animation snapshot" tool, we output .obj models of the animated foot's pose at each observed data frame. These models were then directly measurable in the same way as any other static 3-D foot model. By computing arch variables across multiple trials, we could compare temporal patterns of arch deformation during walking on different substrates.

2.2.2 | Comparing foot arches to track arches

In a second application, which was presented in one of our recent publications (Hatala et al., 2023), we compared the arches of tracks to the arches of the feet that created those tracks. For the latter, we measured arch morphology at midstance while the track was being created. The midstance measurements provided us with another "anatomical" measurement that might vary depending on whether and how a given deformable substrate supported the arch (i.e., impeded vertical arch deformation) while the foot moved through it. This allowed us to evaluate the extent to which the longitudinal arches of tracks resembled the longitudinal arches of the feet that created them.

2.2.3 | Comparing dynamic foot arches to dynamic track arches

Finally, in a third application that was also presented in a recent publication (Hatala et al., 2023), we took dynamic (frame-by-frame) volumetric arch measurements from both feet and tracks, at various timepoints throughout track creation. This was possible using discrete element method (DEM) simulations of substrates deforming in response to foot motions that were captured during *in vivo* experiments. These simulations, and the methods used to carry them out, are explained in detail in another study (Hatala et al., 2021). We have previously demonstrated that these simulations very closely match observed reality and offer valuable tools for understanding how track morphology develops (Falkingham & Gatesy, 2014; Falkingham et al., 2020; Hatala et al., 2021). Simultaneous visualization and quantification of feet and tracks allowed us to understand the process that causes track arches to differ morphologically from the arches of the feet that created them (Hatala et al., 2023). Here, we use these simulation data in order to highlight how the volumetric arch measurement tools presented in the current article were used to pinpoint how and why foot and track arches diverge.

3 | RESULTS

3.1 | Case studies implementing volumetric arch measurement

3.1.1 | Measuring arches of static and dynamic feet

Comparisons of arch volumes from unloaded and weight-bearing feet showed that RAV decreases substantially under the weight-bearing conditions (Table 2). Unloaded foot RAVs ranged from 6.83 to 8.89, while weight-bearing RAVs ranged from 0.84 to 3.00. Within subjects, RAV decreased by between 66.27% and 87.68% during weight-bearing when compared with unloaded conditions.

For dynamic foot analyses, we selected four variables available from our volumetric measurement tool: RAV, pitch, roll, and mid-axis length; and we observed how those aspects of arch morphology changed throughout stance phase while walking on each of four different substrates (rigid carbon fiber and three muds of increasing compliance). We present data from a single subject here, for simple demonstration of this application of the arch measurement tool.

The pattern of RAV over time was very similar when the same subject walked on rigid carbon fiber and on firm mud (Figure 2a). When they walked on softer muds that were 2.5 and 5 cm deep (labeled "wet 2.5" and "wet 5" in Figure 2), RAV remained relatively higher in the early parts of stance phase, before dropping and following patterns similar to those observed on the two firmer substrates from approximately 70% of stance phase onward (Figure 2a). These observations suggest that arch motion and deformation patterns differ during early parts of stance phase across different substrates, but that they converge on a common trajectory while generating propulsive forces later in stance.

Measurements of pitch over time were quite similar across substrates (Figure 2b). In each trial, pitch started out as positive (toes up), stabilized to some extent at an angle close to zero (foot flat), and then switched to negative during the propulsive part of stance phase (toes

TABLE 2 Arches of unloaded and weight-bearing feet in four human subjects.

Subject	Unloaded RAV	Weight-bearing RAV	% change due to weight-bearing
1	8.89	3.00	66.27
2	6.83	0.84	87.68
3	7.69	1.52	80.18
4	6.94	1.32	80.96

Abbreviation: RAV, relative arch volume.

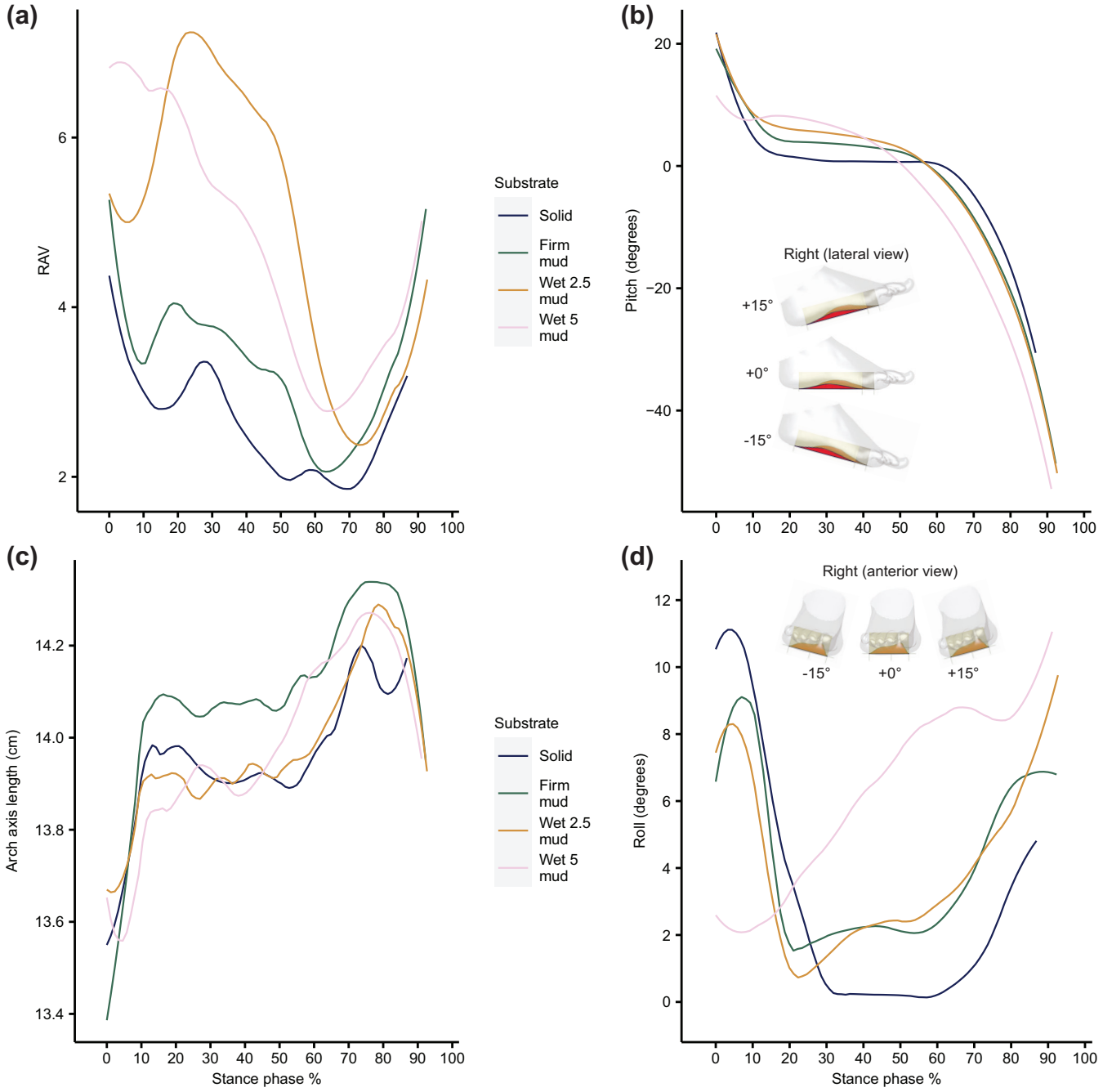

FIGURE 2 Measurements of foot arches during walking on different substrates. A subset of arch model measurements—relative arch volume (RAV) (a), pitch (b), arch axis length (c), and roll (d)—were calculated from frame-by-frame poses of a subject's 3-D animated foot as they walked across four different substrates. The *x*-axes are converted to percentages of stance phase (0–100%) for ease of comparison across trials that differ in their absolute duration. Inset images demonstrate the directions of the pitch and roll axes.

down). Slight variations were apparent, however. When walking on carbon fiber, the subject unsurprisingly experienced a prolonged period of near-zero pitch while the foot was flat on the solid surface. In muds, the heel rose and the forefoot sunk earlier in stance phase. In the deepest mud ("wet 5"), the foot's pitch appeared to never reach a stable, flat position (Figure 2b). There was even a slight increase in pitch in the earliest part of stance on deep mud—soon after heel strike the heel sunk at a faster rate than the rest of the foot. This did not occur on any of the more stable substrates.

The patterns by which the arch lengthened during stance phase were similar across all substrates (Figure 2c), which was surprising given the differences observed for all of the other arch measurements. The arch lengthened early in stance phase (roughly 0%–20% stance phase), stabilized during an intermediate window of time (about 20%–55%), then lengthened again (55%–80%) before rapidly shortening late in propulsion (80% onwards). This subject's arch appeared longer on firm mud than on any other substrate, although it still followed the same temporal pattern that was observed on the others. The scale of

distance between the lines on Figure 2c is quite small (~1.5 mm; equivalent to one bead diameter), however, so we do not make much of this difference. On the deepest mud ("wet 5") arch length began its secondary increase earlier than on any of the other substrates (~45% stance phase; Figure 2c). As with pitch, we attribute this to the lack of stability on this substrate compared with the others, which causes the foot to continue rotating throughout stance rather than finding a true "foot flat" position.

Measurements of roll over time were similar across three of the four substrates, with the deepest mud again being the outlier (Figure 2d). The forefoot everted relative to the hindfoot (roll increased) soon after foot contact, and then leveled out or stabilized once the foot was flat. Roll then increased continuously throughout push-off. On the deepest mud, roll started low and then increased continuously throughout stance phase, never reaching a stable plateau. This may be attributed to this deepest and most pliable mud conceding to the foot's motions rather than resisting them.

3.1.2 | Comparing foot arches to track arches

By measuring the arch of the foot at midstance and then the arch of the track that was formed in each trial, we directly compared the foot's anatomical arch to the arch of the track that the foot left behind. In firm mud, track RAV measurements appear to match closely the RAV measured from feet at midstance (Figure 3). However, we believe this is more coincidental than mechanistically linked—from our video recordings we observed that in most firm mud trials the plantar surface beneath the longitudinal arch never made complete contact with the substrate. The track ended up with a RAV similar to that of the foot because the substrate was displaced during heel strike and toe-off, not because the substrate generated a "mold" of foot anatomy.

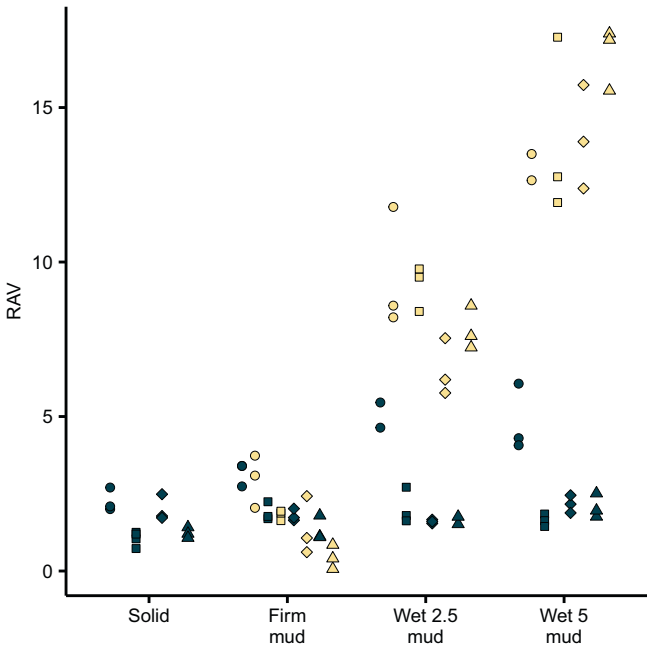

FIGURE 3 Arches of tracks and the feet that produced them. Foot arches (dark green) were measured from 3-D animated feet at midstance in each trial. Track arches (yellow) were measured from 3-D models of the footprints produced in those same trials. The four symbols correspond to four subjects whose data were included here.

In deeper muds, which more closely resemble most known tracks from the human fossil record, track RAV measurements further diverge from those of the feet that created them. In 2.5 cm deep mud ("wet 2.5") track RAV can be two to three times larger than foot RAV; in 5 cm deep mud ("wet 5") tracks can have RAV measurements three to five times larger than the feet that made them (Figure 3). This result emphasizes the mismatch between the arches of tracks and the arch anatomy of the feet that made them.

3.1.3 | Comparing dynamic foot arches to dynamic track arches

By extracting data from particle simulations, our arch measurement tool can also be used to study simultaneous changes to foot and track arches over time (Figure 4). This approach has allowed us to identify when and how track RAV comes to misrepresent foot RAV, and it was essential for determining that track RAV represents a kinematic signal rather than an anatomical one (Hatala et al., 2023).

Track RAV diverges from foot RAV starting just before 50% of stance phase (Figure 4), increasing sharply while foot RAV is instead decreasing. At this time, we can see that the heel is lifting from the substrate. The foot rotates over top of the substrate beneath its longitudinal arch, as the forefoot sinks deeper into the mud. The space that was occupied by the heel and the proximal part of the arch offers a vacant space where substrate can also be pushed backwards and upwards by the forefoot when it exerts propulsive forces (Figure 4). In this way, arch morphology ends up being shaped by the foot's continuous motion as it navigates the deformable substrate, rather than representing a snapshot of static foot anatomy.

4 | DISCUSSION

The case studies presented here demonstrate multiple applications of our volumetric arch measurement tool for quantifying the longitudinal arches of human tracks and human feet. We developed the method with a primary interest in the longitudinal arches of tracks—we wanted to quantify this aspect of 3-D track morphology, which was long considered important but remained difficult to measure. At the same time, we transferred the method to measure 3-D surface models of human feet. We did so to test the hypothesis that a track's longitudinal arch resembles the plantar shape of the foot that created it. Other, perhaps skeletally-based, measurements may still be more appropriate in contexts where researchers' sole objective is to acquire an anatomical measure of longitudinal arch height (e.g., Williams & McClay, 2000). That said, given the increasing use of 3-D foot

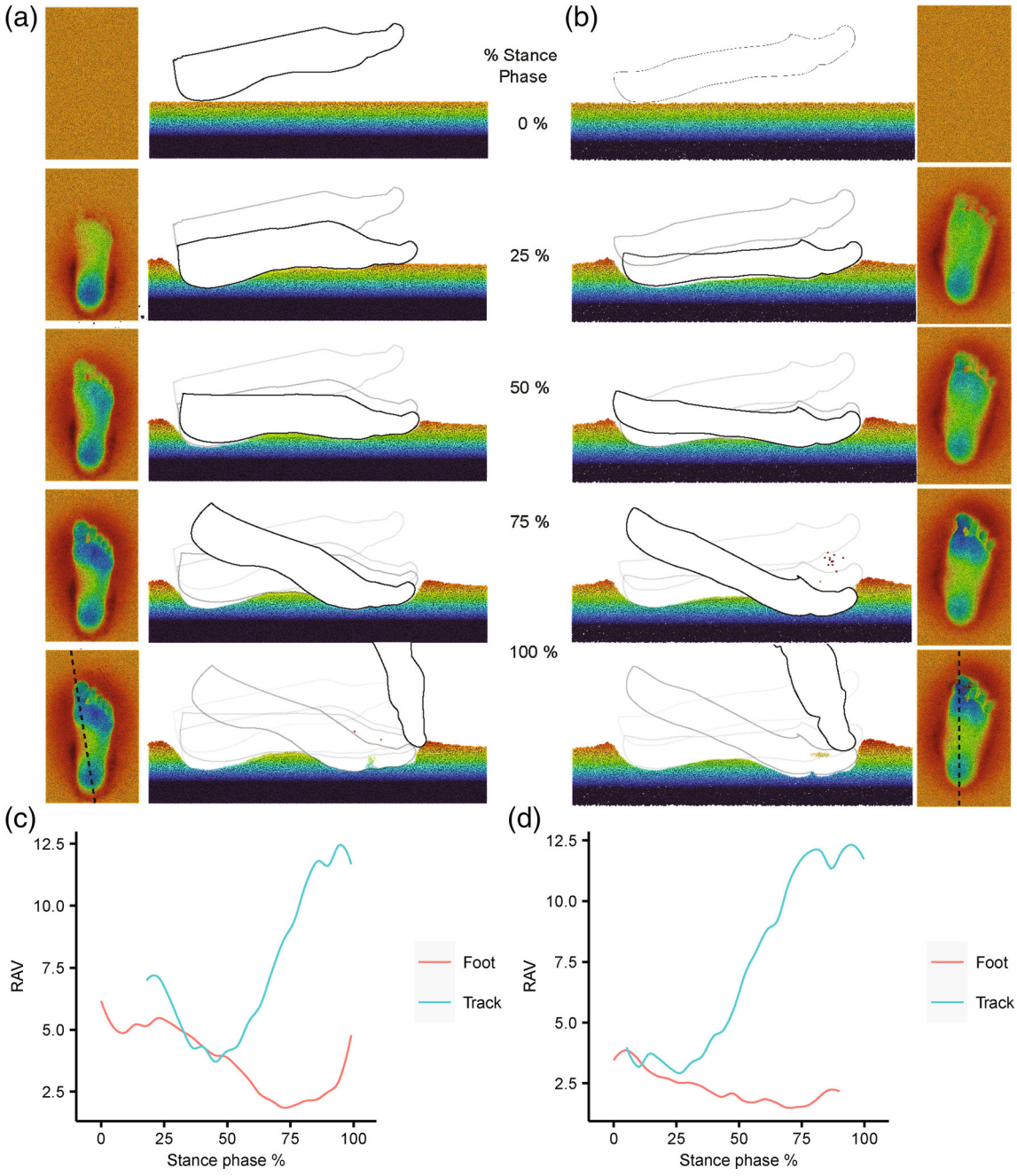

FIGURE 4 Discrete element method (DEM) simulations showing the pattern by which track arches are formed. Subjects with relatively higher (a) and relatively lower arched feet (b) produce tracks with similar longitudinal arches (similar relative arch volume [RAV]) because of the ways their feet move through the deformable substrate. Measurements throughout track simulation show that the arches of tracks sharply diverge from the arches of the feet that made them starting by about 50% stance phase (c, d).

scanners to evaluate arch morphology in living humans (e.g., Schuster et al., 2021; Stanković et al., 2018), our volumetric method (or derivations of it) may be useful for footwear design or for various clinical assessments, for example to track outcomes from surgical interventions that directly treat functional flat-footedness (e.g., Giannini et al., 2001).

The small sample sizes of our case studies mean that we cannot draw generalized conclusions about arch anatomy in modern humans, but we can offer some comparisons with other measurement techniques. Looking first at our static foot measurements in unloaded and weight-bearing conditions (Table 2), we detected percentage decreases in RAV that far exceed decreases observed using 2-dimensional linear and angular arch measurements. For example, Tsung et al. (2003) observed that arch height was about 20% lower, on average, during weight-bearing compared with non-weight-bearing conditions. Williams and McClay (2000) observed even smaller differences (e.g., decreases of 13% for navicular height, and 8% for height of dorsum of foot/truncated foot length) when comparing arch height in

10% and 90% weight-bearing conditions. We observed RAV decreases between 66% and 88%, but perhaps this dramatic difference is not surprising given the contrast between our method and those employed in the other studies. Measuring volumetric changes on the plantar surface of the foot means that our technique will capture external morphological changes that are not captured by, and may have little effect on, linear measurements between the ground and the navicular, or between the ground and the top of the foot. Again, we do not contend that our method is more accurate or more appropriate for all anatomical or functional studies, only that it captures the most relevant information for studying the relationships between tracks and plantar morphology.

Our dynamic arch measurements also afford some opportunities for comparisons with other studies. There have been very few studies of arch deformation on deformable substrates, but Holowka et al. (2018) measured arch deformation on solid substrates in a study of foot stiffness in habitually shod and unshod humans. The dynamic patterns that they observed in longitudinal arch angle, and in changes to longitudinal arch height (Holowka et al., 2018; Figure 3), match well with the patterns that we observed in arch axis length and RAV, respectively, during locomotion on solid substrates (Figure 2). The similarity of these temporal patterns suggests that even if our volumetric arch measurements differ from linear measures in absolute terms, they still capture similar patterns of dynamic changes during locomotion.

As previously described, we developed this volumetric arch measurement tool to directly compare the arches of tracks to the arches of the feet that made them. We first observed that the morphologies of track arches, particularly those made in deep mud, did not match well with direct measurements of the arches of the feet that made them (Figure 3). Using DEM (Kloss & Goniva, 2011; Stukowski, 2010) we conducted experimental data-driven simulations of track formation to examine the foot-substrate interactions that generated the longitudinal arches of tracks (Hatala et al., 2021). From these simulations, we understood that track arches form as a consequence of the foot's heel-sole-toe rollover pattern occurring in a deformable substrate (Figure 4). Thus, a track's arch is a kinematic signal and not an anatomical one (Hatala et al., 2023).

Differences between track and foot arch anatomy are amplified as track depth increases (Figure 3), and most of the known Plio-Pleistocene fossil tracks (e.g., those from Laetoli, Tanzania (Leakey & Hay, 1979) and Ileret, Kenya (Bennett et al., 2009; Hatala et al., 2017)), are sufficiently deep that we expect substantial differences between track and foot arch anatomy. Some other fossil track surfaces even provide data that directly demonstrate that the same individual can produce differently arched tracks, depending on substrate compliance. At Walvis Bay, Namibia, Morse et al. (2013) described substrate-driven differences in track morphology that were observed within trackways produced by the same individuals. In our recent study (Hatala et al., 2023), we also found that the RAVs of tracks made by the same individuals at Walvis Bay increased with relative depth. Because track arches are kinematic signals, and foot kinematics change across substrates of different compliance, the same individuals produced differently arched tracks in areas with different localized substrate conditions (see also Figure 3).

One application not covered here is the comparative analysis of fossil hominin tracks. For such applications we refer the reader to a recent study in which we carried out such analyses (Hatala et al., 2023). However, we wish to draw further attention to one methodological caveat that was described in that study. There we cautioned against blind application of our volumetric arch measurement tool without considering the context in which it is applied. In that study (Hatala et al., 2023), we applied this volumetric measurement technique to chimpanzee tracks, and we showed that arch model geometry is very obviously different from that of a modern human or fossil hominin track. In that case, even though it is feasible to extract a 3-D "arch model" and take various measurements of it (e.g., RAV), those measurements will not be analogous to those from human track arch models, due to the vast differences between chimpanzee and human foot anatomy and kinematics. We do believe that this volumetric measurement tool is robust when analyzing the tracks of hominins who had foot anatomies that are broadly similar to those of modern humans, and who appear to have engaged in patterns of inverted pendular bipedalism (although the method may bring to light potentially important differences in foot kinematics). This includes hominin tracks that may be subtly different from those of modern humans, as our previous analyses (Hatala et al., 2023) have evaluated arch morphologies from Laetoli and Ileret tracks which have slightly more abducted hallux impressions than do the tracks of modern humans (Bennett et al., 2009). We hope that this article provides others with useful tools to carry out similar analyses of hominin tracks from sites that are already known, and from others yet to be discovered.

AUTHOR CONTRIBUTIONS

Kevin G. Hatala: Conceptualization (equal); formal analysis (lead); funding acquisition (equal); investigation (equal); methodology (supporting); project administration (equal); writing – original draft (lead); writing – review and editing (equal). **Stephen M. Gatesy:** Conceptualization (equal); formal analysis (supporting); funding acquisition (equal); investigation (equal); methodology (equal); project administration (equal); software (equal); writing – original draft (supporting); writing – review and editing (equal). **Armita R. Manafzadeh:** Conceptualization (equal); methodology (equal); software (equal); writing – review and editing (equal). **Elizabeth M. Lusardi:** Formal analysis (supporting); investigation (supporting); writing – review and editing (equal). **Peter L. Falkingham:** Conceptualization (equal); formal analysis (supporting); funding acquisition (equal); investigation (equal); methodology (supporting); project administration (equal); software (equal); writing – original draft (supporting); writing – review and editing (equal).

ACKNOWLEDGMENTS

We are grateful to David Baier, Beth Brainerd, Kay Fiske, Kia Huffman, Ben Knörlein, Kyra Tani Little, Sabreen Megherhi, David North, Mahima Sangtani, and Morgan Turner for their assistance directly

related to our biplanar X-ray experiments. We also thank the anonymous volunteers who participated in the X-ray experiments. A PRACE allocation of supercomputer resources (project 2021250007, Irene-Rome) enabled DEM simulations. The study was supported by funding from the National Science Foundation (BCS-1825403 to Kevin G. Hatala and Peter L. Falkingham; BCS-1824821 to Stephen M. Gatesy) and from Chatham University.

CONFLICT OF INTEREST STATEMENT

The authors declare no conflicts of interest.

DATA AVAILABILITY STATEMENT

Scripts for Autodesk Maya and Blender, instructions for using those scripts, and sample animation scenes are all available at the following link: 10.6084/m9.figshare.23585328.

ORCID

Kevin G. Hatala https://orcid.org/0000-0001-9131-5304
Stephen M. Gatesy https://orcid.org/0000-0003-1701-0320
Armita R. Manafzadeh https://orcid.org/0000-0001-5388-7942
Peter L. Falkingham https://orcid.org/0000-0003-1856-8377

REFERENCES

Bennett, M. R., Harris, J. W. K., Richmond, B. G., Braun, D. R., Mbua, E., Kiura, P., Olago, D., Kibunjia, M., Omuombo, C., Behrensmeyer, A. K., Huddart, D., & Gonzalez, S. (2009). Early hominin foot morphology based on 1.5-million-year-old footprints from Ileret, Kenya. *Science*, *323*(5918), 1197–1201. https://doi.org/10.1126/science.1168132

Bennett, M. R., & Morse, S. A. (2014). *Human footprints: Fossilised locomotion?* Springer International Publishing. https://doi.org/10.1007/978-3-319-08572-2

Cavanagh, P. R., & Rodgers, M. M. (1987). The arch index: A useful measure from footprints. *Journal of Biomechanics*, *20*(5), 547–551. https://doi.org/10.1016/0021-9290(87)90255-7

Crompton, R. H., Pataky, T. C., Savage, R., D'Août, K., Bennett, M. R., Day, M. H., Bates, K., Morse, S., & Sellers, W. I. (2012). Human-like external function of the foot, and fully upright gait, confirmed in the 3.66 million year old Laetoli hominin footprints by topographic statistics, experimental footprint-formation and computer simulation. *Journal of the Royal Society Interface*, *9*(69), 707–719. https://doi.org/10.1098/rsif.2011.0258

Day, M. H., & Wickens, E. H. (1980). Laetoli pliocene hominid footprints and bipedalism. *Nature*, *286*(5771), 385–387. https://doi.org/10.1038/286385a0

DeSilva, J. M., & Throckmorton, Z. J. (2010). Lucy's flat feet: The relationship between the ankle and rearfoot arching in early hominins. *PLoS One*, *5*(12), e14432. https://doi.org/10.1371/journal.pone.0014432

Domjanic, J., Seidler, H., & Mitteroecker, P. (2015). A combined morphometric analysis of foot form and its association with sex, stature, and body mass: Morphometric analysis of footprint form. *American Journal of Physical Anthropology*, *157*(4), 582–591. https://doi.org/10.1002/ajpa.22752

Drapeau, M. S. M., & Harmon, E. H. (2013). Metatarsal torsion in monkeys, apes, humans and australopiths. *Journal of Human Evolution*, *64*(1), 93–108. https://doi.org/10.1016/j.jhevol.2012.10.008

Falkingham, P. L., & Gatesy, S. M. (2014). The birth of a dinosaur footprint: Subsurface 3D motion reconstruction and discrete element simulation reveal track ontogeny. *Proceedings of the National Academy of Sciences*, *111*(51), 18279–18284. https://doi.org/10.1073/pnas.1416252111

Falkingham, P. L., Turner, M. L., & Gatesy, S. M. (2020). Constructing and testing hypotheses of dinosaur foot motions from fossil tracks using digitization and simulation. *Palaeontology*, *63*(6), 865–880. https://doi.org/10.1111/pala.12502

Giannini, S., Ceccarelli, F., Benedetti, M. G., Catani, F., & Faldini, C. (2001). Surgical treatment of flexible flatfoot in children: A four-year follow-up study. *The Journal of Bone and Joint Surgery*, *83*(S2), S73–S79.

Hatala, K. G., Demes, B., & Richmond, B. G. (2016). Laetoli footprints reveal bipedal gait biomechanics different from those of modern humans and chimpanzees. *Proceedings of the Royal Society B: Biological Sciences*, *283*(1836), 20160235. https://doi.org/10.1098/rspb.2016.0235

Hatala, K. G., Gatesy, S. M., & Falkingham, P. L. (2021). Integration of biplanar X-ray, three-dimensional animation and particle simulation reveals details of human 'track ontogeny'. *Interface Focus*, *11*(5), 20200075. https://doi.org/10.1098/RSFS.2020.0075

Hatala, K. G., Gatesy, S. M., & Falkingham, P. L. (2023). Arched footprints preserve the motions of fossil hominin feet. *Nature Ecology & Evolution*, *7*(1), 32–41. https://doi.org/10.1038/s41559-022-01929-2

Hatala, K. G., Perry, D. A., & Gatesy, S. M. (2018). A biplanar X-ray approach for studying the 3D dynamics of human track formation. *Journal of Human Evolution*, *121*, 104–118. https://doi.org/10.1016/j.jhevol.2018.03.006

Hatala, K. G., Roach, N. T., Ostrofsky, K. R., Wunderlich, R. E., Dingwall, H. L., Villmoare, B. A., Green, D. J., Braun, D. R., Harris, J. W. K., Behrensmeyer, A. K., & Richmond, B. G. (2017). Hominin track assemblages from Okote Member deposits near Ileret, Kenya, and their implications for understanding fossil hominin paleobiology at 1.5 Ma. *Journal of Human Evolution*, *112*, 93–104. https://doi.org/10.1016/j.jhevol.2017.08.013

Holowka, N. B., & Lieberman, D. E. (2018). Rethinking the evolution of the human foot: Insights from experimental research. *Journal of Experimental Biology*, *221*(17), jeb174425. https://doi.org/10.1242/jeb.174425

Holowka, N. B., Richards, A., Sibson, B. E., & Lieberman, D. E. (2021). The human foot functions like a spring of adjustable stiffness during running. *Journal of Experimental Biology*, *224*, 219667. https://doi.org/10.1242/jeb.219667

Holowka, N. B., Wallace, I. J., & Lieberman, D. E. (2018). Foot strength and stiffness are related to footwear use in a comparison of minimally- vs conventionally-shod populations. *Scientific Reports*, *8*(1), 3679. https://doi.org/10.1038/s41598-018-21916-7

Kelly, L. A., Cresswell, A. G., Racinais, S., Whiteley, R., & Lichtwark, G. (2014). Intrinsic foot muscles have the capacity to control deformation of the longitudinal arch. *Journal of the Royal Society Interface*, *11*(93), 20131188. https://doi.org/10.1098/rsif.2013.1188

Kelly, L. A., Lichtwark, G., & Cresswell, A. G. (2015). Active regulation of longitudinal arch compression and recoil during walking and running. *Journal of the Royal Society Interface*, *12*(102), 20141076. https://doi.org/10.1098/rsif.2014.1076

Kloss, C., & Goniva, C. (2011). LIGGGHTS—Open source discrete element simulations of granular materials based on Lammps. In *TMS2011, 140th Annual Meeting & Exhibition*, San Diego, CA, 27 February–3 March, Suppl. Proc., *Vol. 2, Materials fabrication, properties, characterization, and modeling* (pp. 781–788). John Wiley.

Knörlein, B. J., Baier, D. B., Gatesy, S. M., Laurence-Chasen, J. D., & Brainerd, E. L. (2016). Validation of XMALab software for marker-based XROMM. *Journal of Experimental Biology*, *219*, 3701–3711.

Leakey, M. D., & Hay, R. L. (1979). Pliocene footprints in the Laetoli beds at Laetoli, Northern Tanzania. *Nature*, *278*, 317–323.

McKenzie, R. T. (1909). *Exercise in education and medicine*. W.B. Saunders Company.

Morse, S. A., Bennett, M. R., Liutkus-Pierce, C., Thackeray, F., McClymont, J., Savage, R., & Crompton, R. H. (2013). Holocene footprints in Namibia: The influence of substrate on footprint variability.

American Journal of Physical Anthropology, *151*(2), 265–279. https://doi.org/10.1002/ajpa.22276

Morton, D. J. (1924). Evolution of the longitudinal arch of the human foot. *Journal of Bone and Joint Surgery*, *6*, 56–90.

Prang, T. C. (2015). Rearfoot posture of *Australopithecus sediba* and the evolution of the hominin longitudinal arch. *Scientific Reports*, *5*(1), 17677. https://doi.org/10.1038/srep17677

Schuster, R. W., Cresswell, A., & Kelly, L. (2021). Reliability and quality of statistical shape and deformation models constructed from optical foot scans. *Journal of Biomechanics*, *115*, 110137. https://doi.org/10.1016/j.jbiomech.2020.110137

Stanković, K., Booth, B. G., Danckaers, F., Burg, F., Vermaelen, P., Duerinck, S., Sijbers, J., & Huysmans, T. (2018). Three-dimensional quantitative analysis of healthy foot shape: A proof of concept study. *Journal of Foot and Ankle Research*, *11*(1), 8. https://doi.org/10.1186/s13047-018-0251-8

Stearne, S. M., McDonald, K. A., Alderson, J. A., North, I., Oxnard, C. E., & Rubenson, J. (2016). The foot's arch and the energetics of human locomotion. *Scientific Reports*, *6*(1), 19403. https://doi.org/10.1038/srep19403

Stukowski, A. (2010). Visualization and analysis of atomistic simulation data with OVITO—The open visualization tool. *Modelling and Simulation in Materials Science and Engineering*, *18*, 015012.

Tsung, B. Y. S., Zhang, M., Fan, Y. B., & Boone, D. A. (2003). Quantitative comparison of plantar foot shapes under different weight-bearing conditions. *The Journal of Rehabilitation Research and Development*, *40*(6), 517–526. https://doi.org/10.1682/JRRD.2003.11.0517

Venkadesan, M., Yawar, A., Eng, C. M., Dias, M. A., Singh, D. K., Tommasini, S. M., Haims, A. H., Bandi, M. M., & Mandre, S. (2020). Stiffness of the human foot and evolution of the transverse arch. *Nature*, *579*(7797), 97–100. https://doi.org/10.1038/s41586-020-2053-y

Ward, C. V., Kimbel, W. H., & Johanson, D. C. (2011). Complete fourth metatarsal and arches in the foot of *Australopithecus afarensis*. *Science*, *331*(6018), 750–753. https://doi.org/10.1126/science.1201463

Welte, L., Kelly, L. A., Kessler, S. E., Lieberman, D. E., D'Andrea, S. E., Lichtwark, G. A., & Rainbow, M. J. (2021). The extensibility of the plantar fascia influences the windlass mechanism during human running. *Proceedings of the Royal Society B: Biological Sciences*, *288*(1943), 20202095. https://doi.org/10.1098/rspb.2020.2095

Welte, L., Kelly, L. A., Lichtwark, G. A., & Rainbow, M. J. (2018). Influence of the windlass mechanism on arch-spring mechanics during dynamic foot arch deformation. *Journal of the Royal Society Interface*, *15*(145), 20180270. https://doi.org/10.1098/rsif.2018.0270

Williams, D. S., & McClay, I. S. (2000). Measurements used to characterize the foot and the medial longitudinal arch: Reliability and validity. *Physical Therapy*, *80*(9), 864–871. https://doi.org/10.1093/ptj/80.9.864

SUPPORTING INFORMATION

Additional supporting information can be found online in the Supporting Information section at the end of this article.

How to cite this article: Hatala, K. G., Gatesy, S. M., Manafzadeh, A. R., Lusardi, E. M., & Falkingham, P. L. (2024). Technical note: A volumetric method for measuring the longitudinal arch of human tracks and feet. *American Journal of Biological Anthropology*, 1–11. https://doi.org/10.1002/ajpa.24897